DESIGN OF EQUATION RELATING BOUNDARY CONDITION PARAMETERS AND HEAT TRANSFER COEFFICIENT IN AUTOCLAVE DURING CURING OF COMPOSITE MATERIALS

Thanh Tung Nguyen[1], Anh Quan Tran[1], Truong Le Bich Tram[2], Duc Thang Tran[1], Van Thanh Hoang[1]*

[1]The University of Danang - University of Science and Technology, Vietnam
[2]The University of Danang, Vietnam

*Corresponding author: hvthanh@dut.udn.vn

(Received: May 15, 2025; Revised: June 18, 2025; Accepted: June 21, 2025)

DOI: 10.31130/ud-jst.2025.23(9D).556E

Abstract – In this study, carbon fiber-reinforced composites for aerospace applications were processed in an autoclave under high pressure and temperature. Similar to laboratory conditions, the loading arrangement in each cycle may vary, leading to differences in thermal mass, airflow, and non-uniform temperature distribution, which ultimately affect process stability and product quality. To address this, the heat transfer coefficient (HTC), a key factor in small-scale experimental autoclaves, was analyzed using calorimetric measurements and computational fluid dynamics (CFD) simulations. A turbulent flow model was applied, and HTC was evaluated under different boundary conditions and spatial locations. The results indicated that HTC remained relatively stable, enabling separate assessment of heat transfer and material curing. A design of experiments (DOE) approach was employed to establish an equation relating boundary conditions, spatial positioning, airflow characteristics, and HTC. This equation was validated through comparison with experimental data and Bohne's simulations, confirming its reliability.

Key words – Autoclave; heat transfer coefficient; computational fluid dynamics; finite element method; design of experiments.

1. Introduction

Composites play an increasingly vital role in the aerospace industry, with up to 60% of the components of aircraft and spacecraft made from this type of material. Specifically, composite materials are commonly used to manufacture components such as aircraft frames, fuselages, and wings. In the aerospace sector, composite materials are valued for their strength, high-pressure resistance, lightweight nature, and minimal deformation. These characteristics make composite materials highly utilized in the aerospace industry.

The autoclave process is one of the most common techniques for manufacturing high-performance thermoset structures in the aeronautical and aerospace industries, both for military and commercial applications. In aerospace applications, polymer matrix composites are favored for their excellent specific properties. Carbon fiber–reinforced plastics (CFRP) are particularly attractive because they combine low weight with high mechanical performance, including strength, fatigue resistance, and corrosion-free behavior, making them superior to conventional aerospace alloys. CFRPs are employed in a broad spectrum of aerospace components, ranging from primary load-bearing structures like wings and fuselages to secondary parts including seats and floor panels. Looking ahead, their use is expected to expand to advanced applications such as engine components, particularly with the development of PAN-based carbon fibers of medium elasticity [1].

The primary manufacturing process currently employed involves the layup of prepreg material using automated tape layers, followed by curing the components in an autoclave under elevated pressure and temperature. This method achieves a high level of compaction and low porosity. The autoclave cycle is characterized by slow heating rates ranging from 0.5 K/min to 2.5 K/min, reaching a maximum temperature of 180°C. A standard cure cycle typically lasts 7 to 14 hours [1] to ensure complete curing and avoid overheating damage from the exothermic reaction.

The conservative processing parameters account for the variability of autoclave loading, which differs between cycles when multiple CFRP components are cured simultaneously. This variability results in differing thermal masses and airflow patterns inside the autoclave [2]. To optimize cure cycles for shorter durations, it is crucial to understand the temperature distribution within the CFRP part. Several mechanisms affect this distribution, including convection from the heated autoclave air, heat transfer from the tooling, and conduction through the composite material [1]. The final cure state therefore depends on the time-varying temperature field within the component.

In manufacturing, temperature measurements of CFRP parts are typically temperature- and pressure-dependent. Furthermore, these measurements are highly influenced by the location of the CFRP part within the autoclave, which is characterized by a three-dimensional airflow pattern determined by the design of the autoclave itself. While numerous studies have focused on the effect of curing cycle temperature on the temperature distribution within composite parts, relatively little attention has been given to the influence of the mold on this temperature field. To address this gap, an improved curing process has been proposed to achieve better uniformity in the temperature distribution of the composite product.

Weber et al. [3] reviewed the key parameters affecting convective HTC in mold panels and introduced a thermal simulation method based on shift factors combined with a reference curve. Their approach, however, was limited to

simple mold geometries of different sizes. Consequently, reducing temperature gradients in small laboratory autoclaves remains essential [4].

Antonucci et al. [5] focused on two parameters that define the heat transfer phenomena between the carrying energy fluid and the tooling-composite element in industrial autoclave technology: the global heat exchange coefficient H and the adiabatic temperature rise ΔT_a. The study revealed that autoclave technology is governed by two dimensionless parameters: Ω, the ratio between the processing time and the convective time, is generally higher than unity to minimize the temperature variation, and Ξ, the ratio between the reaction time and the convective time, representing the contribution of the reaction heat dissipation to the part's temperature profile.

Preglej et al. [6] carried out the mathematical model based on heat transfer and pressure variation theories relevant to autoclave processes, including heating, cooling, and pressure changes. The results indicated that the designed model is applicable for the development of various process control strategies, including advanced univariate and multivariate control algorithms.

Kluge et al. [7] examined three different settings by varying the inlet pressure conditions and the rate of temperature increase while maintaining stable low air velocity. The findings highlighted the critical role of convection, which elucidates issues related to non-homogeneous flow inside autoclaves. Particle Image Velocimetry (PIV) is particularly important, as it can be employed to optimize uniform heating. Additionally, the researchers observed that the applied pressure increased the estimated average HTC by approximately 2.6 times compared to an autoclave run without applied pressure.

Zhang et al. [8] developed a large-framed mold, considering convective heat transfer and turbulence within the autoclave. The results demonstrated that the thermal properties of both the mold and the fluid significantly influence the heating performance. For the fabrication of large-framed molds, steel and copper are preferable due to their enhanced temperature field distributions. Moreover, blending gases like helium or argon with air has been proposed as a way to enhance heat transfer inside autoclaves, thereby improving the heating efficiency of large molds and ensuring better quality in large composite structures.

Tobias Bohne et al. [2] showed a range of models for analyzing heat transfer in CFRP (Carbon Fiber Reinforced Polymer) parts during the curing process. These models vary from simple 1D representations with constant temperature distributions to more complex analytical models based on calorimeter measurements of heat transfer in the autoclave. Advanced fluid dynamics calculations are also utilized to characterize airflow patterns, ultimately aiding in predicting the degree of cure and optimizing cure cycles for specific loadings. Additionally, understanding the degree of cure and temperature distribution allows for predicting process-induced distortions in CFRP parts, which depend on the transient temperature variations within the material.

Through research, those authors have observed that no existing research paper has established an equation or a clear relationship between the HTC and the boundary conditions applied to the composite component. By employing computational simulations and the design of experiments methodology, the authors have developed an equation that defines this relationship based on a set of equations from previous studies, which describe the interactions between boundary condition parameters in two different cases. Furthermore, the obtained results were compared with Tobias Bohne's research to evaluate the HTC values at different locations within the autoclave, thereby enabling practical application in real-world scenarios.

2. Theoretical basic

2.1. Empirical formular

Define The experiment was carried out in a small laboratory autoclave with a working area of 2 m in length and 1 m in diameter. According to the manufacturer's specifications, the ventilator delivers a volumetric flow rate of 1.04 m^3/s. Under this assumption, the HTC for the mass calorimeter can be determined using the relation in [1, 9]:

$$h = \frac{mc_p\frac{dT}{dt}}{(T_\infty - T)\cdot A} \quad (1)$$

Where m represents the mass of the aluminum plate, c_p denotes the specific heat capacity of the aluminum plate, T_∞ is the temperature of the liquid environment within the autoclave, T indicates the inner surface temperature recorded by the calorimeter, and A is the total free surface area of both the upper and lower sides of the aluminum plate [2].

Furthermore, the convective HTC for various types of autoclaves, when using a calorimeter, has been predicted by Johnston et al. [1] as shown in the equation. In this equation, C is an empirical constant that is unique to each autoclave. The value of C can be determined based on the diameter and central axis of the autoclave:

$$h = C\left(\frac{P}{T}\right)^{\frac{4}{5}}\frac{W}{m^2K} \quad (2)$$

For a specific geometry, the Reynolds number of the fluid is directly proportional to the fluid's average velocity and density and inversely proportional to the absolute viscosity of the gas [10]. The relationship between the Reynolds number (Re) and the Nusselt number (Nu) for fully developed turbulent flow is expressed in the following equation:

$$Nu \infty Re^{\frac{4}{5}} \infty \frac{h}{k} \quad (3)$$

The heating process of the mold is carried out through forced convection of the fluid; therefore, the flow type must be considered. The flow is turbulent and can be characterized by the Reynolds number (R_e), where ρ is the density of the fluid, V is the average velocity of the fluid, L is the characteristic length, ν is the kinematic viscosity of the fluid, and μ is the dynamic viscosity of the fluid.

$$R_e = \frac{\rho V L}{\mu} = \frac{V L}{\nu} \quad (4)$$

By employing analytical equations for pipe flow, the inlet Reynolds number is calculated as $Re_{inlet} = 9.3e + 4$, which is much higher than the transition threshold for turbulence, typically $Re_{crit} = 2300$. This leads to the assumption that the flow has fully developed into the turbulent regime [1]. From this, the relationship linking turbulent viscosity to molecular viscosity is obtained as:

$$\frac{\eta_T}{\eta} = 10 \quad (5)$$

this results in a kinematic viscosity coefficient of $2.7e-5\ m^2 s^{-1}$ under the inlet conditions.

The Grashof number (Gr) is a dimensionless parameter that approximates the ratio of buoyant forces to viscous forces acting on a fluid. Typically, a decrease in density with increasing temperature causes the fluid to rise, a motion induced by buoyancy [11]. The Grashof number is the key parameter used to quantify these opposing forces:

$$Gr = \frac{g.\beta.(|T_s - T_\infty|).L^3}{\nu^2} \quad (6)$$

Where g is the gravitational acceleration, β is the thermal expansion coefficient of the fluid, T_s is the surface temperature, T_∞ is the ambient fluid temperature, L is the characteristic dimension of the system, and ν is the kinematic viscosity of the fluid.

The Prandtl number (Pr) is a dimensionless quantity defined as the ratio of momentum diffusivity to thermal diffusivity [12]. It is expressed by the following equation:

$$Pr = \frac{\nu}{\alpha} = \frac{c_p \mu}{k} \quad (7)$$

Where c_p is the specific heat capacity at constant pressure, μ represents the dynamic viscosity, and k denotes the thermal conductivity.

Based on the empirical equations reviewed above, an experimental equation was investigated in the following study. The research was conducted under two cases, drawing upon the results of Bohne's scientific paper for both the experimental and simulated outcomes in terms of the HTC.

Case 1: Formulation based on Forced Convection.

$$HTC = C.R_e{}^x.P_r{}^y.G_r{}^z.P_{outlet}{}^t \quad (8)$$

Case 2: Formulation based on Natural Convection.

$$HTC = C.R_e{}^a.P_{outlet}{}^b.Gr^c \quad (9)$$

2.2. Design of experiment method

Experimental design is an innovative research approach in which mathematical tools play a crucial role, relying on statistical probability theory based on variance analysis and regression analysis [13]. This method was originally proposed by R. Fisher in the 1930s in his work *Design of Experiments*.Since theoretical equations cannot fully capture the input–output relationships, the processes or research objects are modeled as a "black box," as illustrated in the following Figure 1 [13].

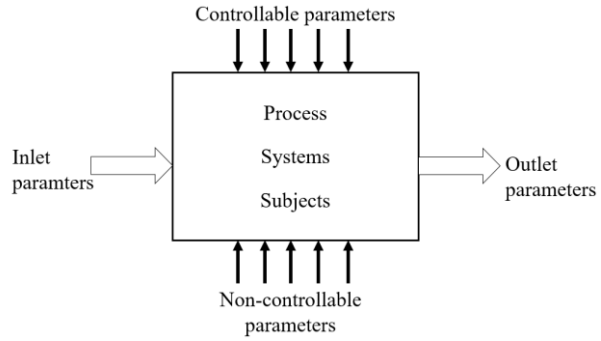

Figure 1. *Experimental Design Research Model*

A multiple regression equation is employed to analyze the factors influencing the output quantity, which depends on several input variables, in the form of a regression model [13]. The equation is expressed as follows:

$$\begin{cases} y_1 = b_0x_{01} + b_1x_{11} + \cdots + b_kx_{k1} \\ y_2 = b_0x_{02} + b_1x_{12} + \cdots + b_kx_{k2} \\ \cdots\cdots\cdots\cdots \\ y_n = b_0x_{0n} + b_1x_{1n} + \cdots + b_kx_{kn} \end{cases} \quad (10)$$

Case 1: For the experimental scenario based on Bohne's experiment.

$$\ln(h) = \ln(C) + x\ln(R_e) + y\ln(P_r) + z\ln(Gr) + t\ln(P_{outlet}) \quad (11)$$

The function can be rewritten in the following form:

$$H_1 = B_0 + x.X_1 + y.X_2 + z.X_3 + t.X_4$$

With: $H_1 = \ln(h)$, $B_0 = \ln(C)$, $X_1 = \ln(R_e)$, $X_2 = \ln(P_r)$, $X_3 = \ln(G_r)$, $X_4 = \ln(P_{outlet})$

Case 2: For the simulation scenario based on Bohne's results.

$$\ln(h) = \ln(C) + a\ln(R_e) + b\ln(P_{outlet}) + c\ln(Gr) \quad (12)$$

The function can be rewritten in the following form:

$$H_2 = B_1 + a.Y_1 + b.Y_2 + c.Y_3$$

With: $H_2 = \ln(h)$, $B_1 = \ln(C)$, $Y_1 = \ln(R_e)$, $Y_2 = \ln(P_{outlet})$, $Y_3 = \ln(Gr)$.

3. Simulation

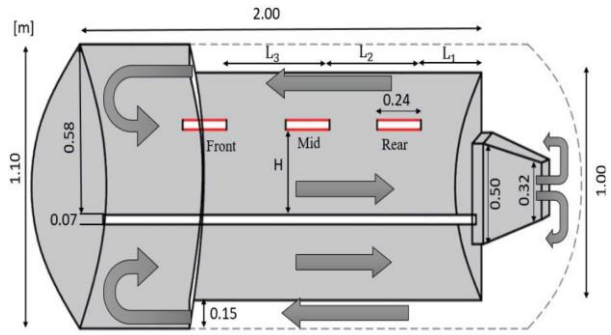

Figure 1. *Airflow in the Autoclave*

The operating principle of an experimental autoclave is illustrated in the Figure 2. In the diagram, the direction of the hot air flow is indicated by arrows [1]. Hot air is drawn from the autoclave's door into the working chamber, where a constant temperature difference is observed between the

calorimeter surface and the liquid temperature within the autoclave [2]. Subsequently, the hot air exits the autoclave through the door, and the tools along with the composite components are heated by the circulating hot air.

3.1. Geometric method and mesh

To analyze the spatial distribution of the convective HTC within the autoclave, a block calorimeter is positioned at three locations along the central axis of the autoclave: front, mid, and rear, as illustrated in the Figure 3.

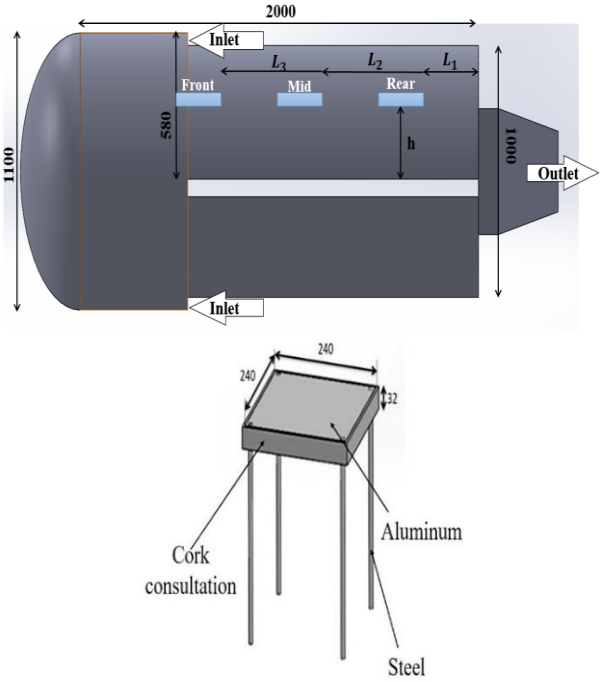

Figure 2. *Geometric simulation model (unit: mm)*

The simulation geometric model used during the simulation process is illustrated in Figure 4. This model includes a small-scale laboratory autoclave and a structured aluminum plate, designed based on technical specifications and direct measurements when data were not available.

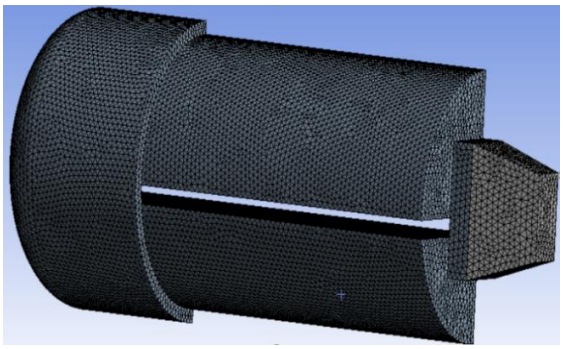

Figure 3. *Mesh model in Ansys simulation*

Given the complex geometry of the model and the need to reduce CPU processing time, a symmetric model was constructed with elements of uniform size. In the conjugate heat transfer process between the liquid and solid phases, the mesh conditions at the interface between the two phases affect the accuracy of the simulation. The computational mesh for the model is divided into an unstructured mesh (triangular grid), with a refined mesh density in the sliding regions of the model.

After conducting simulations using coarse, medium, and fine mesh types, the authors observed that the simulation results remained unchanged when the fine mesh was applied. The corresponding mesh parameters are summarized in the following Table 1.

Table 1. *Calculation mesh parameters.*

Type of grid	Elements	Nodes
Triangles	818528	160737

Therefore, the mesh parameters for the remaining cases were generated using triangular elements with a 'fine' mesh setting to ensure mesh convergence while minimizing computational time across different mesh configurations for the various cases.

3.2. Boundary conditions and solver

Based on the real operating conditions of the laboratory autoclave, a simplified simulation model was constructed, as illustrated in Figure 5.

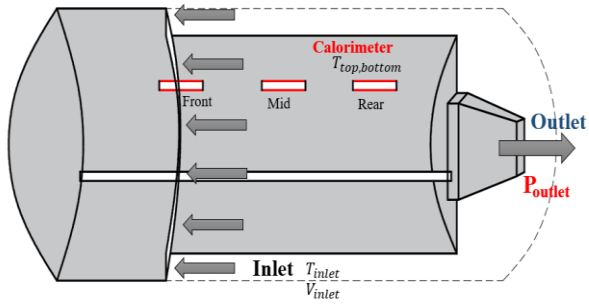

Figure 4. *Autoclave conditions and placement in simulation*

The inlet velocity was modeled as uniform, with its velocity calculated from the fan's volumetric flow rate and inlet area [4], and the direction assumed normal to the inlet surface. Using the convective heat transfer model, the finite volume method in Fluent 21.1 was applied to predict the temperature field. The boundary condition parameters adopted for the design are summarized in Table 2.

Table 2. *Boundary condition parameters*

Case	L(m)	V_{inlet} (m/s)	P_{outlet} (bar)	T_{inlet} (°K)	T_s (°K)	T_∞ (°K)
1	$L_1 = 0.34$ $L_2 = 0.87$ $L_3 = 1.27$	8	10	333.15	328.15	321.15
2	$L_1 = 0.36$ $L_2 = 0.88$ $L_3 = 1.28$	5	4	333.15	324.15	321.15
3	$L_1 = 0.33$ $L_2 = 0.86$ $L_3 = 1.35$	4	8	331.15	324.15	321.15
4	$L_1 = 0.31$ $L_2 = 0.85$ $L_3 = 1.3$	10	5	331.15	330.15	321.15
5	$L_1 = 0.33$ $L_2 = 0.86$ $L_3 = 1.35$	6	9	330.15	324.15	321.15

In this case, the Spalart – Allmaras (SA) turbulence model was applied to the fluid region in the simulation. The

SA model is a one-equation RANS model that is particularly suited for aerospace applications. At the inlet, a uniform velocity profile was prescribed, determined from the ratio of the fan's volumetric flow rate to the inlet cross-sectional area. The flow direction was set normal to the inlet plane [1]. This model offers high stability and efficiency in simulating moderately attached and separated flows, making it widely used in aerodynamic studies. It also allows for high resolution in near-wall regions, facilitating an accurate simulation of the thermal boundary layer [7]. A time – dependent iterative solver was used for the calculation. A time step of 0.05 s was selected based on stability and accuracy requirements. The simulation was run until t = 15 s, which was sufficient for the system to reach a steady – state condition.

In this study, the gas flow conditions within the autoclave were maintained at 55°C and 7 bar [2]. Consequently, different conditions of the gas flow's characteristic parameters, along with the properties of various materials, were considered in this case to accurately determine the simulation results and material properties such as those of steel, insulating materials, and aluminum, as illustrated in the Table 3.

Table 3. *Material properties in simulations*

Material properties	Gas at 55°C and 7bar	Aluminum	Insulation Material	Steel
Density (kg/m^3)	7.4326	2719	200	7850
Conducitity (W/m.K)	0.0286	202.4	0.045	16.27
Specific heat (J/kg.K)	1015.7	871	350	350
Dynamic viscosity (Pa.s)	1.9948e-5	-	-	-

4. Result and discussion

After performing simulations for five different cases with the corresponding boundary conditions shown in Table 1 and material property parameters listed in Table 2, the resulting HTC for each case are presented in Table 4.

Table 4. *Simulation results of HTC*

Case	L(m)	HTC
1	$L_1 = 0.34$	48.46
	$L_2 = 0.87$	59.03
	$L_3 = 1.27$	88.15
2	$L_1 = 0.36$	29.04
	$L_2 = 0.88$	39.25
	$L_3 = 1.28$	55.71
3	$L_1 = 0.33$	44.79
	$L_2 = 0.86$	57.7
	$L_3 = 1.35$	79.45
4	$L_1 = 0.31$	31.57
	$L_2 = 0.85$	37.44
	$L_3 = 1.3$	60.81
5	$L_1 = 0.33$	36.89
	$L_2 = 0.86$	48.31
	$L_3 = 1.35$	84.68

By applying the design of experiment method using the equations (8) and (9), we obtained the following expressions for the HTC in terms of the parameters for both cases:

Case 1: Formulation based on Forced Convection.

$$\mathrm{HTC} = 0{,}0197.P_{outlet}{}^{0,5902}.\left(\frac{V_{inlet}.L}{\nu}\right)^{-0,734}.\left(\frac{\mu.c_p}{k}\right)^{-35,4492}.\left(\frac{g.(T_s-T_\infty).L^3}{\nu^2.T_{inlet}}\right)^{0,36953} \quad (13)$$

Case 2: Formulation based on Natural Convection.

$$HTC = e^4.\left(\frac{V_{inlet}.L}{\nu}\right)^{0,2902}.\left(\frac{\mu.c_p}{k}\right)^{16}.P_{outlet}{}^{0,5154} \quad (14)$$

After obtaining equations (13) and (14), we evaluated their reliability and found that Equation (13) has a coefficient of determination of $R^2 = 0.979211$,while Equation (14) has $R^2 = 0.750367$ Both equations demonstrate high reliability and can therefore be used to predict the HTC based on the boundary conditions during the curing process of composite materials in the autoclave.

Based on the relationship between the equations for both cases, and in conjunction with the simulation results as well as Bohne's experimental findings, the obtained values are presented in Figure 6.

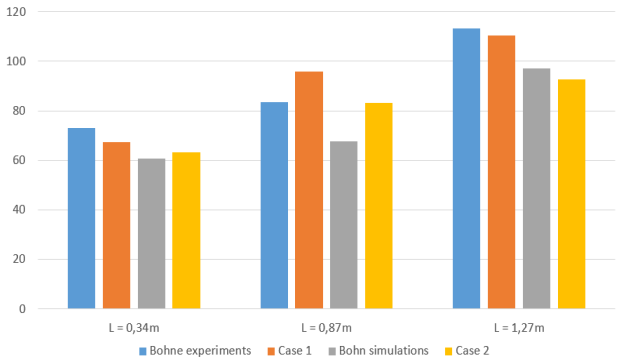

Figure 6. *Comparison results between two cases and the simulation-experiment results of Bohne*

From this, the errors for both cases were determined. It was observed that Case 1 yielded results closely approximating Bohne's experimental findings, whereas Case 2 produced outcomes that aligned well with Bohne's simulations as shown in [2]. Accordingly, the error results for both cases are presented in the Figure 7.

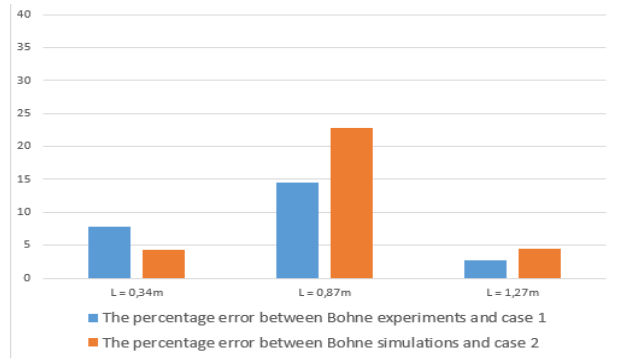

Figure 7. *The percentage error between Case 1 and Bohne's experiment, and between Case 2 and Bohne's simulation*

The comparison indicates that the HTC gradually decreases from the front to the rear of the autoclave. With a uniform distribution of temperature and static pressure in the numerical simulation, the HTC values can accurately represent the flow field in the autoclave's digital model, despite some observable complexities. Notably, heat transfer is significantly higher in the front region. This comparison also reveals minor differences among Bohne's experimental results, his simulations, and the two equations from the new simulation cases. It can be observed that the percentage error at the three positions L = 0.34 m and L = 1.27 m is below 10%, while the error at L = 0.87 m is relatively around 20%, which may be attributed to the poorly defined temperature distribution in the central region is not well-defined. This is due to the simultaneous influence of the inlet temperature and outlet pressure, which causes significant variations in the simulation results. Consequently, the Equation fails to accurately reflect the conditions in this highly disturbed region. Additionally, the influence of geometric convective flow introduces the effects of secondary vortices and flow reversal phenomena, further contributing to the discrepancy in the simulation at this location.

After evaluating Equations (13) and (14), the authors suggest that Equation (14) is suitable for cases involving a stable operating temperature range, where temperature variations within the autoclave are negligible under practical conditions. In contrast, Equation (13) is recommended for scenarios with significant temperature fluctuations, as it accounts for comprehensive variations in boundary conditions within the autoclave.

5. Conclusion

In this study, the objective was to develop an equation that describes the relationship between boundary condition parameters and the heat transfer coefficient (HTC) inside a small-scale laboratory autoclave used for the processing of composite materials. To achieve this, we investigated the HTC under five different scenarios, considering variations in inlet velocity, outlet pressure, mold position, and operating temperatures. The finite volume method was employed to determine the HTC values corresponding to these five conditions. Based on these results, two theoretical equations were developed to describe the relationship between the boundary conditions and the HTC using the Design of Experiments (DOE) approach.

From the simulation results across the five cases, it was observed that the closer the mold is positioned to the air inlet, the higher the HTC becomes, and vice versa. Therefore, to improve curing efficiency-especially for large molds that require high curing temperatures-it is recommended to place them closer to the air inlet. Conversely, smaller molds with lower curing temperature requirements can be positioned near the outlet of the autoclave.

The authors have developed two equations correlating the HTC with the boundary conditions. These equations can serve as references during the composite curing process to estimate the HTC of a mold inside the autoclave. This allows for HTC prediction under varying boundary conditions without requiring additional experimental measurements or flow simulations inside the autoclave, thereby optimizing the curing performance.

Between equations (13) and (14), the authors recommend using Equation (13) in situations where significant temperature variations occur within the autoclave, as it provides better accuracy. In contrast, when the autoclave flow does not involve substantial changes in inlet or initial temperatures, Equation (14) is more suitable for predicting the HTC during the curing process of composite materials.

Acknowledgment: This research is funded by Ministry of Education and Training, Vietnam, under project number B2024.DNA.17.

REFERENCES

[1] M. Hudek, M. Shewfelt, and R. M. Shead, "Examination of heat transfer in autoclaves", in *Proc. 46th Int. SAMPE Symp. and Exhibition*, Long Beach, California, USA, 2001.

[2] T. Bohne, T. Frerich, J. Jendrny, J.-P. Jurgens, and V. Ploshikhin, "Temperature modeling in autoclave processes", *J. Compos. Mater*., vol. 1–11, Oct. 2017.

[3] T. A. Weber and J. Arent, "A fast method of the generation of boundary conditions for thermal autoclave simulation", *Compos. Part A: Appl. Sci. Manuf*., vol. 88, pp. 216–225, Sep. 2016.

[4] N. Han, L. An, L. Fan, L. Hua, and G. Gao, "Research on temperature field distribution in a frame mould during autoclave process", *Biomed Res. Int*., vol. 13, no. 18, p. 4020, Sep. 2020.

[5] V. Antonucci *et al.,* "Analysis of heat transfer in autoclave technology", *Res. Gate*, vol. 22, no. 5, pp. 613–620, Oct. 2001.

[6] A. Preglej *et al.*, "Mathematical model of an autoclave", *Res. Gate*, vol. 57, no. 6, pp. 503–516, Jan. 2011.

[7] N. E. J. Kluge *et al*., "An experimental study of temperature distribution in an autoclave", *J. Reinf. Plast. Compos*., vol. 35, no. 7, Jan. 2016.

[8] G. Z. Guowei, Z. Boming, L. Ling, L. Ting, and X. Xiangchen, "Influence of mould and heat transfer fluid materials on the temperature distribution of large framed moulds in autoclave process", *Biomed Res. Int*., vol. 14, no. 15, p. 4311, Aug. 2021.

[9] N. Ersoy and T. Garstka, "Modeling of the spring-in phenomenon in curved parts made of a thermosetting composite", *Compos. Part A: Appl. Sci. Manuf*., vol. 41, no. 3, pp. 410–418, Mar. 2010.

[10] M. Hudek, Examination of heat transfer during autoclave processing of polymer composites, *M.Sc. Thesis, Univ. of Manitoba*, Canada, 2001.

[11] R. B. Bird, W. E. Stewart, and E. N. Lightfoot, *Transport Phenomena, 2nd ed.,* New York: John Wiley & Sons, 2002.

[12] J. M. Coulson and J. F. Richardson, *Chemical Engineering*, Vol. 1, 6th ed., Oxford: Butterworth-Heinemann, 1999.

[13] L. D. Binh, *Design of Experiments in Mechanical Engineering*, Construction Publishing House, 2017.